AIAA SciTech Forum
8–12 January 2018, Kissimmee, Florida
2018 AIAA Guidance, Navigation, and Control Conference

10.2514/6.2018-1125

Retrospective Cost Adaptive Control of the Generic Transport Model Under Abrupt Faults

Ahmad Ansari† and Dennis S. Bernstein††

Aerospace Engineering Department, University of Michigan, 1320 Beal Ave., Ann Arbor, MI 48109

Retrospective cost adaptive control (RCAC) was demonstrated in[1] using the NASA GTM under conditions of uncertainty and failure. In the present paper the goal is to stress RCAC by considering faults that are abrupt, severe, unknown, and unforeseen. In particular, we consider 1) abrupt changes in the aircraft mass properties; 2) abrupt changes in the aerodynamic coefficients; 3) abrupt control-surface deflection and jam; and 4) abrupt thrust failure. Particular attention is paid to the severity of the transient response between the abrupt failure and recovery of the aircraft.

Nomenclature

u	=	input
y	=	measurement
z	=	performance variable
k_0	=	relative degree of the controller
n_c	=	order of the controller
θ	=	controller coefficients
ϕ	=	feedback vector
G_f	=	filter transfer function applied to ϕ and u
$\mathbf{z}$	=	Z-transform
R_z	=	performance penalty
R_θ	=	controller-coefficient penalty
R_u	=	control penalty
V_{AC}	=	airspeed
τ	=	turn rate
h	=	altitude
$\boldsymbol{T}$	=	throttle
$\boldsymbol{e}$	=	elevator
$\boldsymbol{a}$	=	ailerons
$\boldsymbol{r}$	=	rudder
y_{trim}	=	measurement at trim flight
δy	=	measurement increment from trim flight

†Ph.D. Candidate, Aerospace Engineering Department, University of Michigan, Ann Arbor. ansahmad@umich.edu
††Professor, Aerospace Engineering Department, University of Michigan, Ann Arbor. dsbaero@umich.edu

$\delta y_{\rm cmd}$	=	incremental command from trim flight
i	=	channels 1,2,3,4 for $\boldsymbol{T}$, $\boldsymbol{e}$, $\boldsymbol{a}$, and $\boldsymbol{r}$, respectively
$u_{i,\rm trim}$	=	$i^{\rm th}$ constant actuator setting for the trim flight
$\delta u_{i,\rm req}$	=	$i^{\rm th}$ requested actuator setting increment specified by the adaptive controller
$u_{i,\rm req}$	=	$i^{\rm th}$ requested actuator setting
$\delta u_{i,\rm actual}$	=	$i^{\rm th}$ actual actuator setting increment
$u_{i,\rm actual}$	=	$i^{\rm th}$ actual actuator setting

I. Introduction

Although feedback control can perform stabilization, command following, and disturbance rejection, model errors can lead to performance degradation and possibly instability. Classical feedback control of aircraft has been widely studied,[2–4] and state-space-based optimal control techniques have extensively applied.[5,6] Aircraft flight control has also benefited from advances in robust control.[7,8]

Adaptive control techniques[9–14] provide the means for controlling aircraft under emergency flight conditions. The Honeywell MH-96 self-adaptive controller, which failed on the X-15-3, was analyzed in.[13] More recently, L_1 adaptive control was flight tested on the NASA AirStar scaled aircraft.[14]

Using the NASA GTM model, retrospective cost adaptive control (RCAC) was applied to the nominal aircraft as well as unknown off-nominal conditions.[1] RCAC is a direct, discrete-time adaptive control technique for stabilization, command following, and disturbance rejection.[15] As a discrete-time approach, RCAC is motivated by the desire to implement control algorithms that operate at the sensor sample rate without the need for controller discretization. This also means that the required modeling information can be estimated based on data sampled at the same rate as the control update.

RCAC was originally motivated by the notion of retrospectively optimized control, where past controller coefficients used to generate past control inputs are re-optimized in the sense that if the re-optimized coefficients had been used over a previous window of operation, then the performance would have been better. Unlike signal processing applications such as estimation and identification, however, it is impossible to change past control inputs, and thus the re-optimized controller coefficients are used only to generate the next control input.

RCAC was originally developed within the context of active noise control experiments.[16] The algorithm used in[16] is gradient-based, where the gradient direction and step size are based on different cost functions. In subsequent work,[17] the gradient algorithm was replaced by batch least-squares optimization. In both[16] and,[17] the modeling information is given by Markov parameters (impulse response components) of the open-loop transfer function G_{zu} from the control input u to the performance variable z. More recently, in,[18] a recursive least squares (RLS) algorithm was used, along with knowledge of the NMP zeros of G_{zu}. The approaches in[16–18] are closely related in the sense that all of the NMP zeros outside of the spectral radius of G_{zu} are approximate zeros of a polynomial whose coefficients are Markov parameters of G_{zu}; this polynomial is a truncated Laurent expansion of G_{zu} about infinity. RCAC uses a filter $G_{\rm f}$ to define the retrospective cost by filtering the difference between the actual past control inputs and the re-optimized control inputs. To construct $G_{\rm f}$, Markov parameters are used in,[16,17,19] and NMP zeros are used in.[18,20]

More recently,[15] RCAC was reinterpreted as a residual-minimization technique involving the transfer function between a virtual control input and the performance variable. In particular, it was shown in[15] that the filter $G_{\rm f}$ used to define the retrospective performance variable provides a target model for an intercalated transfer function. In effect, RCAC updates the controller coefficients so as to fit the intercalated transfer function to the target model. This mechanism supports the principle underlying RCAC. The fact that the target model $G_{\rm f}$ requires limited modeling information (primarily sign and NMP zeros) makes it possible to

apply RCAC to highly uncertain plants.

The goal of the present paper is to expand the study of RCAC in.[1] As in,[1] we interface RCAC with the NASA GTM simulation model.[21–24] This aircraft model includes an aerodynamic data base, trim function, and interface to facilitate feedback control from realistic sensors to thrust and control surfaces. For RCAC, which operates at a fixed sample rate, A/D and D/A operations are implemented through Simulink blocks. The present paper goes beyond[1] by focusing on the case where the aircraft is subject to faults that are abrupt, severe, unknown, and unforeseen. Without further adaptation, these faults may lead to extreme performance degradation and possibly instability. Consequently, RCAC must adapt quickly in order to recover stability and attain the best achievable post-fault performance. The goal of this paper is thus to investigate the ability of RCAC to recover stability and performance under faults that are abrupt, severe, unknown, and unforeseen.

The investigation in this paper is based on several case studies involving abrupt, severe, unknown, and unforeseen faults. In all examples, GTM is initially in steady level flight, and RCAC is used to trim the aircraft. The scenarios that are considered include a change in the aircraft mass and mass distribution; changes in the aerodynamic coefficients; faulty control surfaces; and thrust failure. For all examples, RCAC uses the same tuning parameters; this restriction is consistent with the assumption that the faults are unknown and unforeseen.

II. RCAC Algorithm

II.A. Plant Model

Consider the MIMO discrete-time system

$$x(k+1) = Ax(k) + Bu(k) + D_1 w(k), \tag{1}$$

$$y(k) = Cx(k) + D_2 w(k), \tag{2}$$

$$z(k) = E_1 x(k) + E_0 w(k), \tag{3}$$

where $x(k) \in \mathbb{R}^{l_x}$ is the state, $y(k) \in \mathbb{R}^{l_y}$ is the measurement, $u(k) \in \mathbb{R}^{l_u}$ is the input, $w(k) \in \mathbb{R}^{l_w}$ is the exogenous signal, and $z(k) \in \mathbb{R}^{l_z}$ is the performance variable. The goal is to develop an adaptive output feedback controller that minimizes z in the presence of the exogenous signal w with limited modeling information about (1)–(3). The components of w can represent either command signals to be followed, external disturbances to be rejected, or both, depending on the choice of D_1 and E_0. This formulation defines the signals that play a role in RCAC. However, no assumptions are made concerning the state space realization since RCAC requires input-output model information rather than details of the state space realization.

II.B. The Controller

Define the dynamic compensator

$$u(k) = \sum_{i=1}^{n_c} P_i(k)u(k-i) + \sum_{i=k_0}^{n_c} Q_i(k)\xi(k-i), \tag{4}$$

where $P_i(k) \in \mathbb{R}^{l_u \times l_u}, Q_i(k) \in \mathbb{R}^{l_u \times l_\xi}$ are the controller coefficient matrices, $k_0 \geq 0$, and $\xi(k) \in \mathbb{R}^{l_\xi}$ consists of components of y, z, and w. We rewrite (4) as

$$u(k) = \phi(k)\theta(k), \tag{5}$$

where the regressor matrix $\phi(k)$ is defined by

$$\phi(k) \triangleq \begin{bmatrix} u(k-1) \\ \vdots \\ u(k-n_{\mathrm{c}}) \\ \xi(k-k_0) \\ \vdots \\ \xi(k-n_{\mathrm{c}}) \end{bmatrix}^{\mathrm{T}} \otimes I_{l_u} \in \mathbb{R}^{l_u \times l_\theta} \tag{6}$$

and

$$\theta(k) \triangleq \mathrm{vec} \begin{bmatrix} P_1(k) \cdots P_{n_{\mathrm{c}}}(k) \; Q_{k_0}(k) \cdots Q_{n_{\mathrm{c}}}(k) \end{bmatrix} \in \mathbb{R}^{l_\theta}, \tag{7}$$

where $l_\theta \triangleq l_u^2 n_{\mathrm{c}} + l_u l_\xi (n_{\mathrm{c}} + 1 - k_0)$, "$\otimes$" is the Kronecker product, and "vec" is the column-stacking operator. Note that $k_0 = 0$ yields an exactly proper controller, whereas $k_0 \geq 1$ yields a strictly proper controller.

II.C. Retrospective Performance Variable

We define the retrospective control as

$$\hat{u}(k) = \phi(k)\hat{\theta} \tag{8}$$

and the corresponding retrospective performance variable as

$$\hat{z}(k) \triangleq z(k) + \phi_{\mathrm{f}}(k)\hat{\theta} - u_{\mathrm{f}}(k), \tag{9}$$

where $\hat{\theta} \in \mathbb{R}^{l_\theta}$ is determined by optimization below, and $\phi_{\mathrm{f}}(k) \in \mathbb{R}^{l_z \times l_\theta}$, and $u_{\mathrm{f}}(k) \in \mathbb{R}^{l_z}$ are filtered versions of $\phi(k)$, and $u(k)$, respectively, defined by

$$\phi_{\mathrm{f}}(k) \triangleq G_{\mathrm{f}}(\mathbf{q})\phi(k), \tag{10}$$

$$u_{\mathrm{f}}(k) \triangleq G_{\mathrm{f}}(\mathbf{q})u(k). \tag{11}$$

The filter G_{f} has the form

$$G_{\mathrm{f}}(\mathbf{q}) \triangleq D_{\mathrm{f}}^{-1}(\mathbf{q})N_{\mathrm{f}}(\mathbf{q}), \tag{12}$$

where D_{f} and N_{f} are polynomial matrices, and D_{f} is asymptotically stable and monic. The choice of the filter is discussed in the next section.

II.D. Construction of G_{f}

In,[17,25–28] the filter G_{f} is based on the Markov parameters of the control-to-performance transfer matrix G_{zu}. In particular, for all complex numbers z whose absolute value is greater than the spectral radius of A, it follows that

$$G_{zu}(\mathbf{q}) = E_1(\mathbf{q}I - A)^{-1}B = \sum_{i=0}^{\infty} \frac{H_i}{\mathbf{q}^i}, \tag{13}$$

where, for all, $i \geq 1$, the i^{th} Markov parameter of G_{zu} is defined by

$$H_i \triangleq E_1 A^{i-1} B. \tag{14}$$

Truncating (13) yields G_{f} given by the $n_{\mathrm{f}}^{\mathrm{th}}$-order Markov parameter-based FIR filter

$$G_{\mathrm{f}}(\mathbf{q}) = \sum_{i=1}^{n_{\mathrm{f}}} \frac{H_i}{\mathbf{q}^i}. \tag{15}$$

In,[15] G_{f} is shown to provide a target model for the intercalated transfer function between the virtual control perturbation and z. This interpretation leads to guidelines for constructing G_{f} in terms of limited modeling data that consists of the leading signs, relative degree, and NMP zeros of G_{zu}.

II.E. Retrospective Cost Function

Using the retrospective performance variable $\hat{z}(k)$, we define the retrospective cost function

$$J(k,\hat{\theta}) \triangleq \sum_{i=1}^{k} [\hat{z}^{\mathrm{T}}(i) R_z \hat{z}(i) + (\phi(i)\hat{\theta})^{\mathrm{T}} R_u(i) \phi(i)\hat{\theta}] + (\hat{\theta} - \theta(0))^{\mathrm{T}} R_\theta (\hat{\theta} - \theta(0)), \tag{16}$$

where R_z and R_θ are positive definite, and, for all $i \geq 1$, $R_u(i)$ is positive definite.

Proposition 1: Let $P(0) = R_\theta^{-1}$. Then, for all $k \geq 1$, the retrospective cost function (16) has a unique global minimizer $\theta(k)$, which is given by

$$\theta(k) = \theta(k-1) - P(k-1)\tilde{\phi}(k)^{\mathrm{T}} \Gamma(k)^{-1} [\tilde{\phi}(k)\theta(k-1) + \tilde{z}(k)], \tag{17}$$

$$P(k) = P(k-1) - P(k-1)\tilde{\phi}(k)^{\mathrm{T}} \Gamma(k)^{-1} \tilde{\phi}(k) P(k-1), \tag{18}$$

where

$$\tilde{\phi}(k) \triangleq \begin{bmatrix} \phi_{\mathrm{f}}(k) \\ \phi(k) \end{bmatrix} \in \mathbb{R}^{(l_\xi + l_u) \times l_\theta}, \tag{19}$$

$$\tilde{R}(k) \triangleq \begin{bmatrix} R_z & 0 \\ 0 & R_u(k) \end{bmatrix} \in \mathbb{R}^{(l_\xi + l_u) \times (l_\xi + l_u)}, \tag{20}$$

$$\tilde{z}(k) \triangleq \begin{bmatrix} z(k) - u_{\mathrm{f}}(k) \\ 0 \end{bmatrix} \in \mathbb{R}^{l_\xi + l_u}, \tag{21}$$

$$\Gamma(k) \triangleq \tilde{R}(k)^{-1} + \tilde{\phi}(k) P(k-1) \tilde{\phi}(k)^{\mathrm{T}}. \tag{22}$$

III. RCAC Control Architecture for the GTM

To apply RCAC to GTM, we define a decentralized adaptation structure, where, for each component of the performance variable z in (3), a separate RCAC block has a scalar output u given by (4). Sensor signals are shared among the channels in order to account for channel coupling.

Let V_{AC}, h, τ, and β denote the airspeed, altitude, turn rate, and sideslip angle, respectively. The aircraft control inputs are $\boldsymbol{T}$, $\boldsymbol{e}$, $\boldsymbol{a}$, and $\boldsymbol{r}$, which denote throttle, elevator, ailerons, and rudder, respectively. We use the index $i = 1, 2, 3, 4$ to denote the channels for $\boldsymbol{T}$, $\boldsymbol{e}$, $\boldsymbol{a}$, $\boldsymbol{r}$, respectively.

We define the measurement increments in each channel as

$$\delta V_{\mathrm{AC}}(k) \triangleq V_{\mathrm{AC}}(k) - V_{\mathrm{AC,trim}}, \tag{23}$$

$$\delta h(k) \triangleq h(k) - h_{\mathrm{trim}}, \tag{24}$$

$$\delta \tau(k) \triangleq \tau(k) - \tau_{\mathrm{trim}}, \tag{25}$$

$$\delta \beta(k) \triangleq \beta(k) - \beta_{\mathrm{trim}}, \tag{26}$$

where the subscript "trim" refers to the initial trim flight, and k denotes the current time step. We choose the sample time to be 0.1 sec which is approximately 7.86 times the frequency (in Hz) of the short period mode of GTM trimmed in horizontal flight at airspeed 100.59 kt and altitude 8000 ft. The performance variable z is given by the error signals

$$z(k) \triangleq \begin{bmatrix} V_{\mathrm{AC}}(k) - V_{\mathrm{AC,cmd}}(k) \\ h(k) - h_{\mathrm{cmd}}(k) \\ \tau(k) - \tau_{\mathrm{cmd}}(k) \\ \beta(k) - \beta_{\mathrm{cmd}}(k) \end{bmatrix} = \begin{bmatrix} \delta V_{\mathrm{AC}}(k) - \delta V_{\mathrm{AC,cmd}}(k) \\ \delta h(k) - \delta h_{\mathrm{cmd}}(k) \\ \delta \tau(k) - \delta \tau_{\mathrm{cmd}}(k) \\ \delta \beta(k) - \delta \beta_{\mathrm{cmd}}(k) \end{bmatrix}, \tag{27}$$

where $V_{\mathrm{AC,cmd}}$, γ_{cmd}, τ_{cmd}, and β_{cmd} are the commands, and

$$\delta V_{\mathrm{AC,cmd}} \triangleq V_{\mathrm{AC,cmd}} - V_{\mathrm{AC,trim}}, \tag{28}$$

$$\delta h_{\mathrm{cmd}} \triangleq h_{\mathrm{AC,cmd}} - h_{\mathrm{AC,trim}}, \tag{29}$$

$$\delta \tau_{\mathrm{cmd}} \triangleq \tau_{\mathrm{AC,cmd}} - \tau_{\mathrm{AC,trim}}, \tag{30}$$

$$\delta \beta_{\mathrm{cmd}} \triangleq \beta_{\mathrm{AC,cmd}} - \beta_{\mathrm{AC,trim}} \tag{31}$$

$$\tag{32}$$

are the incremental commands. Note that all increments are defined relative to the initial trim.

Let the requested actuator settings be denoted by

$$\boldsymbol{T}_{\mathrm{req}}(k) \triangleq \boldsymbol{T}_{\mathrm{trim}} + \delta \boldsymbol{T}_{\mathrm{req}}(k), \tag{33}$$

$$\boldsymbol{e}_{\mathrm{req}}(k) \triangleq \boldsymbol{e}_{\mathrm{trim}} + \delta \boldsymbol{e}_{\mathrm{req}}(k), \tag{34}$$

$$\boldsymbol{a}_{\mathrm{req}}(k) \triangleq \boldsymbol{a}_{\mathrm{trim}} + \delta \boldsymbol{a}_{\mathrm{req}}(k), \tag{35}$$

$$\boldsymbol{r}_{\mathrm{req}}(k) \triangleq \boldsymbol{r}_{\mathrm{trim}} + \delta \boldsymbol{r}_{\mathrm{req}}(k), \tag{36}$$

where the first term on the right-hand side denotes the constant actuator setting for the initial trim, and the second term on the right-hand side denotes the requested actuator setting increment specified by RCAC. The actual actuator settings are determined by the actuator dynamics, which are modeled as first-order systems with saturation nonlinearities modeled by stroke and rate limits;[24,29] the parameters of the actuator models are given in Table 1. Thus, the requested actuator settings may not be equal to the actual actuator settings,

Table 1: Parameters of the actuator models for the throttle, elevator, ailerons, and rudder.

	Stroke Limits	**Rate Limits**	**Bandwidth**
Throttle $\boldsymbol{T}$	[0, 100%]	∞	20π Hz
Elevator $\boldsymbol{e}$	[−20 deg, 30 deg]	[−300 deg/sec, 300 deg/sec]	20π Hz
Ailerons $\boldsymbol{a}$	[−20 deg, 20 deg]	[−300 deg/sec, 300 deg/sec]	20π Hz
Rudder $\boldsymbol{r}$	[−30 deg, 30 deg]	[−300 deg/sec, 300 deg/sec]	20π Hz

which are denoted by

$$\boldsymbol{T}_{\text{actual}}(k) \triangleq \boldsymbol{T}_{\text{trim}} + \delta\boldsymbol{T}_{\text{actual}}(k), \tag{37}$$

$$\boldsymbol{e}_{\text{actual}}(k) \triangleq \boldsymbol{e}_{\text{trim}} + \delta\boldsymbol{e}_{\text{actual}}(k), \tag{38}$$

$$\boldsymbol{a}_{\text{actual}}(k) \triangleq \boldsymbol{a}_{\text{trim}} + \delta\boldsymbol{a}_{\text{actual}}(k), \tag{39}$$

$$\boldsymbol{r}_{\text{actual}}(k) \triangleq \boldsymbol{r}_{\text{trim}} + \delta\boldsymbol{r}_{\text{actual}}(k), \tag{40}$$

where the left-hand side denotes the actual actuator setting, and the second term on the right-hand side denotes the actual actuator setting increment.

For each channel, RCAC updates a strictly proper dynamic controller represented in input-output form as

$$\delta u_{i,\text{req}}(k) = \phi_i(k)^{\text{T}}\theta_i(k), \tag{41}$$

where $\delta u_{i,\text{req}}$ denotes the requested actuator setting increment for the ith channel, where, for example, the corresponding actuator in the ith channel is $\delta\boldsymbol{T}_{\text{req}}$, $\delta\boldsymbol{e}_{\text{req}}$, $\delta\boldsymbol{a}_{\text{req}}$, and $\delta\boldsymbol{r}_{\text{req}}$ for $i = 1, 2, 3, 4$, respectively. For channel i, the components of the feedback vector ϕ_i include values of the actual actuator setting increment $u_{i,\text{actual}}$, which is $\delta\boldsymbol{T}_{\text{actual}}$, $\delta\boldsymbol{e}_{\text{actual}}$, $\delta\boldsymbol{a}_{\text{actual}}$, and $\delta\boldsymbol{r}_{\text{actual}}$ for $i = 1, 2, 3, 4$, respectively, as well as additional signals

$$\begin{aligned}
\phi_1(k) \triangleq [\, &\delta\boldsymbol{T}_{\text{actual}}(k-1) \cdots \delta\boldsymbol{T}_{\text{actual}}(k-n_{\text{c}}) \quad \delta V_{\text{AC,cmd}}(k-1) \cdots \delta V_{\text{AC,cmd}}(k-n_{\text{c}}) \\
&z_1(k-1) \cdots z_1(k-n_{\text{c}}) \qquad \delta h(k-1) \cdots \delta h(k-n_{\text{c}})]^{\text{T}}, \\
\phi_2(k) \triangleq [\, &\delta\boldsymbol{e}_{\text{actual}}(k-1) \cdots \delta\boldsymbol{e}_{\text{actual}}(k-n_{\text{c}}) \quad \delta h_{\text{cmd}}(k-1) \cdots \delta h_{\text{cmd}}(k-n_{\text{c}}) \\
&z_2(k-1) \cdots z_2(k-n_{\text{c}}) \qquad \delta V_{\text{AC}}(k-1) \cdots \delta V_{\text{AC}}(k-n_{\text{c}})]^{\text{T}}, \\
\phi_3(k) \triangleq [\, &\delta\boldsymbol{a}_{\text{actual}}(k-1) \cdots \delta\boldsymbol{a}_{\text{actual}}(k-n_{\text{c}}) \quad \delta\tau_{\text{cmd}}(k-1) \cdots \delta\tau_{\text{cmd}}(k-n_{\text{c}}) \\
&z_3(k-1) \cdots z_3(k-n_{\text{c}}) \qquad \delta\beta(k-1) \cdots \delta\beta(k-n_{\text{c}})]^{\text{T}}, \\
\phi_4(k) \triangleq [\, &\delta\boldsymbol{r}_{\text{actual}}(k-1) \cdots \delta\boldsymbol{r}_{\text{actual}}(k-n_{\text{c}}) \quad \delta\beta_{\text{cmd}}(k-1) \cdots \delta\beta_{\text{cmd}}(k-n_{\text{c}}) \\
&z_4(k-1) \cdots z_4(k-n_{\text{c}}) \qquad \delta\tau(k-1) \cdots \delta\tau(k-n_{\text{c}})]^{\text{T}},
\end{aligned} \tag{42}$$

where $z = [z_1\ z_2\ z_3\ z_4]^{\text{T}}$ and z_1, z_2, z_3, z_4 are the components of z in (27), which is the vector of command-following errors. The vector θ_i of controller coefficients has the same size as ϕ_i. Figure 1 shows the block diagram for channel 1, which uses thrust to follow the airspeed command. In doing so, it uses airspeed command as a feedforward signal, airspeed command-following error as a feedback signal, and altitude as coupling feedback signals. The remaining channels use similar structures to follow altitude, turn-rate, and sideslip-angle commands.

IV. Parameters for RCAC Control of GTM Under Abrupt Changes

At the start of each example, the aircraft is assumed to be flying in an initial trim without the use of feedback control. The components of the controller coefficient vector θ are thus initially set to zero, that is, $\theta(0) = 0$. Although $\theta(0)$ can be set arbitrarily, we choose $\theta(0) = 0$ to reflect the absence of additional modeling information. RCAC must therefore adapt the components of θ from their initial zero values to suitable nonzero values. To assist in the transition from open-loop to closed-loop control, in all examples, we introduce zero-mean white noise with standard deviation 0.001% into $\boldsymbol{T}_{\text{req}}$ and zero-mean white noise with standard deviation 0.001 deg into $\boldsymbol{e}_{\text{req}}$, $\boldsymbol{a}_{\text{req}}$, and $\boldsymbol{r}_{\text{req}}$ from $t = 10$ sec to $t = 70$ sec. Unless stated otherwise, for all of the examples considered in this paper, we use

$$G_{\text{f}}(\mathbf{z}) = \text{diag}(1/\mathbf{z}^4, -1/\mathbf{z}^4, -1/\mathbf{z}^4, 1/\mathbf{z}^4).$$

Since GTM is a nonlinear model, the guidelines for choosing G_{f} given in[15] cannot be used directly. The entries of G_{f} are thus chosen based on the numerical response of the GTM model under nominal conditions.

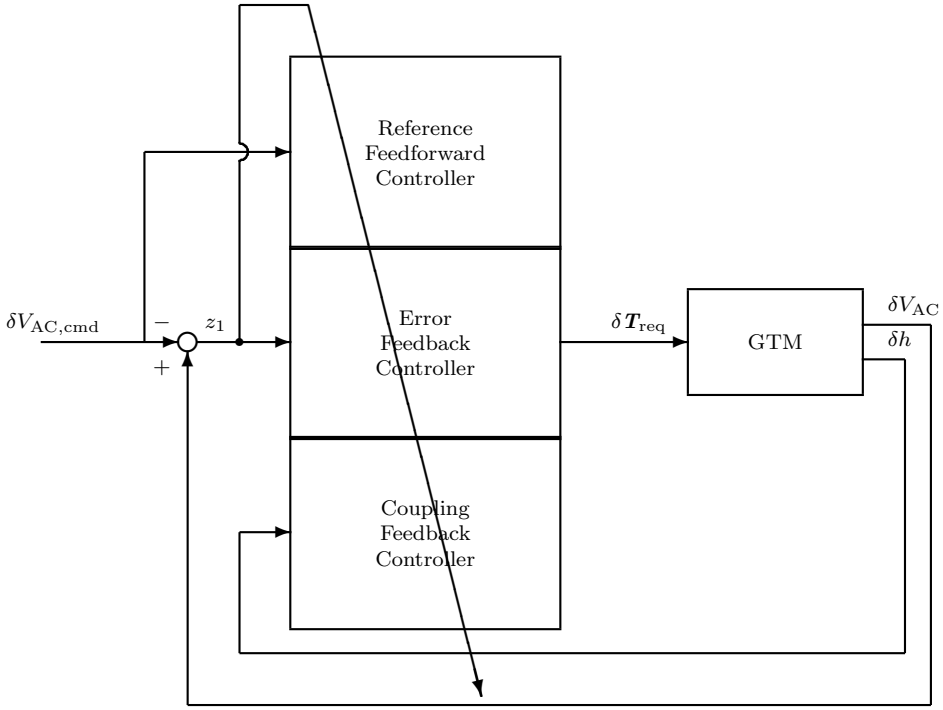

Figure 1. Block diagram for channel 1, which uses thrust to follow the airspeed command. The error signal z_1 for the control is the difference $\delta V_{\mathrm{AC,cmd}} - \delta V_{\mathrm{AC}}$. This channel also uses altitude increment for feedback.

In addition, for all examples, we use identical tuning parameters; consequently, no special tuning is used for particular examples in this paper. This restriction respects the assumption that the abrupt changes considered in later subsections are unmodeled and unanticipated, and therefore the control law cannot be tuned or tailored for the collection of failures that are considered. The tunings that are used for all examples are given by $n_{\mathrm{c}} = 8$, $R_z = I_4$, $R_\theta = \mathrm{diag}(10^{-4} I_{4n_{\mathrm{c}}}, 10^{-1} I_{4n_{\mathrm{c}}}, 10^{-2} I_{4n_{\mathrm{c}}}, 10^{-3} I_{4n_{\mathrm{c}}})$, and

$$R_u(k) = \begin{cases} \mathrm{diag}(g(z_1(k), 16, 4, 1, 0.01), g(z_2(k), 900, 1, 10, 0.1), \\ \qquad g(z_3(k), 1, 0.01, 10, 1), g(z_4(k), 0.01, 0.0025, 10, 1)), & k \le 700, \\ \mathrm{diag}(0.01, 1, 0.1, 1), & k > 700, \end{cases}$$

$$g(z(k), z_{\mathrm{high}}, z_{\mathrm{low}}, R_{u,\mathrm{high}}, R_{u,\mathrm{low}}) \triangleq \begin{cases} R_{u,\mathrm{high}}, & z^2(k) > z_{\mathrm{high}}, \\ m(z^2(k) - z_{\mathrm{low}}), & z_{\mathrm{low}} + \bar{z} \le z^2(k) \le z_{\mathrm{high}}, \\ R_{u,\mathrm{low}}, & z^2(k) < z_{\mathrm{low}} + \bar{z}, \end{cases}$$

where $m \triangleq \frac{R_{u,\mathrm{high}}}{z_{\mathrm{high}} - z_{\mathrm{low}}}$ and $\bar{z} \triangleq \frac{R_{u,\mathrm{low}}}{R_{u,\mathrm{high}}}(z_{\mathrm{high}} - z_{\mathrm{low}})$. Note that g increases linearly as a function of z^2 within the interval $[z_{\mathrm{low}}, z_{\mathrm{high}}]$. Furthermore, note that R_u is constant beginning at $t = 70\,\mathrm{sec}$, which is the end of the initial adaptation.

Unless stated otherwise, for all of the examples in this paper, GTM is initialized with the trim

$$\begin{gathered} V_{\mathrm{AC}}(0) = V_{\mathrm{AC,trim}} = 100.6\,\mathrm{kt},\ \gamma(0) = \gamma_{\mathrm{trim}} = 0\ \mathrm{deg},\ \tau(0) = \tau_{\mathrm{trim}} = 0\,\mathrm{deg/sec}, \\ \beta(0) = \beta_{\mathrm{trim}} = 0\,\mathrm{deg},\ \alpha(0) = \alpha_{\mathrm{trim}} = 3\ \mathrm{deg},\ h(0) = 8000\,\mathrm{ft}. \end{gathered} \tag{43}$$

The initial deflections of all actuators are set to the values corresponding to this initial trim, namely,

$$\begin{gathered} \boldsymbol{T}_{\mathrm{actual}}(0) = \boldsymbol{T}_{\mathrm{trim}} = 22.8\%,\ \boldsymbol{e}_{\mathrm{actual}}(0) = \boldsymbol{e}_{\mathrm{trim}} = 2.7\ \mathrm{deg}, \\ \boldsymbol{a}_{\mathrm{actual}}(0) = \boldsymbol{a}_{\mathrm{trim}} = 0\ \mathrm{deg},\ \boldsymbol{r}_{\mathrm{actual}}(0) = \boldsymbol{r}_{\mathrm{trim}} = 0\ \mathrm{deg}\,. \end{gathered}$$

V. Abrupt Changes in the Mass Properties

We now consider several scenarios where the dynamics of the aircraft change abruptly during flight in an unknown way. We first consider changes in the aircraft mass properties, namely, the aircraft mass, moments of inertia, and center-of-gravity (cg) location. For all of the examples in this section, the center of pressure (cp) and cg are initially colocated; however, the cp and cg are distinct after the changes occur.

Example 1. Straight-line flight with constant altitude and airspeed command. The incremental commands are given by

$$\delta V_{\mathrm{AC,cmd}}(k) = 0\,\mathrm{kt},\ \delta h_{\mathrm{cmd}}(k) = 0\,\mathrm{ft},\ \delta\tau_{\mathrm{cmd}}(k) = 0\,\mathrm{deg/sec},\ \delta\beta_{\mathrm{cmd}}(k) = 0\,\mathrm{deg}. \tag{44}$$

At $t = 100\,\mathrm{sec}$, the cg abruptly moves forward by 1.14 inch. Since the cg moves forward, this change is not destabilizing; the opposite situation is considered in Example 2.

Figures 2(c), 2(f), 2(i), and 2(l) show that θ converges after the initial adaptation, and subsequently brings the aircraft back to its initial trim at $t = 90\,\mathrm{sec}$ with zero command-following errors for airspeed, altitude, turn rate, and sideslip angle. Figure 2(f) shows that, at $t = 100\,\mathrm{sec}$, the elevator controller coefficients readapt due to the resulting change in dynamics, and the aircraft continues straight-line flight with constant airspeed and altitude. At $t = 250\,\mathrm{sec}$, the command-following errors for airspeed, altitude, turn rate, and sideslip angle are 0.1 kt, 1.37 ft, 0.02 deg/sec, and 0.0003 deg, respectively.

Example 2. Horizontal circular flight with trapezoidal airspeed and turn-rate commands. The incremental commands are given by

$$\begin{gathered}\delta V_{\mathrm{AC,cmd}}(k) = \begin{cases} 0, & k < 1000, \\ \max\{-10, -0.01(k-1000)\}\,\mathrm{kt}, & k \geq 1000, \end{cases} \\ \delta\tau_{\mathrm{cmd}}(k) = \begin{cases} 0, & k < 1000, \\ \min\{5, 0.005(k-1000)\}\,\mathrm{deg/sec}, & k \geq 1000, \end{cases} \\ \delta h_{\mathrm{cmd}}(k) = 0\,\mathrm{ft},\ \delta\beta_{\mathrm{cmd}}(k) = 0\,\mathrm{deg}. \end{gathered} \tag{45}$$

At $t = 250\,\mathrm{sec}$, the cg abruptly moves aft by 1.15 inch.

Figure 3 shows that, after the initial adaptation, the maximum command-following errors for airspeed, altitude, turn rate, and sideslip angle are 3.54 kt, 9.56 ft, 2.41 deg/sec, and 0.18 deg, respectively. Figure 3(f) shows that, at $t = 250\,\mathrm{sec}$, the elevator controller coefficients readapt due to the resulting change in dynamics, and the aircraft continues horizontal circular flight with constant airspeed and altitude. At $t = 350\,\mathrm{sec}$, the command-following errors for airspeed, altitude, turn rate, and sideslip angle are 0.1 kt, 0.35 ft, 0.002 deg/sec, and 0.10 deg, respectively. Note that the requested actuator settings in all four channels become constant after 280 sec.

Example 3. Horizontal circular flight with trapezoidal airspeed and turn-rate commands. The incremental commands are given by

$$\begin{gathered}\delta V_{\mathrm{AC,cmd}}(k) = \begin{cases} 0, & k < 1000, \\ \max\{-10, -0.01(k-1000)\}\,\mathrm{kt}, & k \geq 1000, \end{cases} \\ \delta\tau_{\mathrm{cmd}}(k) = \begin{cases} 0, & k < 1000, \\ \min\{5, 0.005(k-1000)\}\,\mathrm{deg/sec}, & k \geq 1000, \end{cases} \\ \delta h_{\mathrm{cmd}}(k) = 0\,\mathrm{ft},\ \delta\beta_{\mathrm{cmd}}(k) = 0\,\mathrm{deg}. \end{gathered} \tag{46}$$

At $t = 250\,\mathrm{sec}$, the cg is abruptly moved forward by 1.14 inch, and the mass and moments of inertia are abruptly decreased. The initial mass and moments of inertia of GTM are 1.54 slug and [1.32, 4.25, 5.4, 0.1125] lbf-ft^2/sec, respectively. At 250 sec, the mass decreases by 0.1 slug, and the moments of inertia $[I_{xx}, I_{yy}, I_{zz}, I_{xz}]$ decrease by [0.083, 0.26, 0.34, 0.0075] lbf-ft^2/sec.

Figure 4 shows that, after the initial adaptation, the maximum command-following errors for airspeed, altitude, turn rate, and sideslip angle are 3.55 kt, 11.84 ft, 1.32 deg/sec, and 0.14 deg, respectively. Figure 4(f) shows that, at $t = 250$ sec, the elevator controller coefficients readapt due to the resulting change in dynamics, and the aircraft continues horizontal circular flight with constant airspeed and altitude. At $t = 350$ sec, the command-following errors for airspeed, altitude, turn rate, and sideslip angle are 0.01 kt, 2.8 ft, 0.002 deg/sec, and 0.10 deg, respectively. Note that the requested actuator settings in all four channels become constant after 280 sec.

Example 4. Straight-line flight with constant airspeed and trapezoidal altitude commands. The incremental commands are given by

$$\begin{gathered}\delta h_{\rm cmd}(k) = \begin{cases} 0, & k < 1000, \\ \min\{100, 0.1(k-1000)\}\,\text{ft}, & k \geq 1000, \end{cases} \\ \delta V_{\rm AC,cmd}(k) = 0\,\text{kt},\ \delta\tau_{\rm cmd}(k) = 0\,\text{deg/sec},\ \delta\beta_{\rm cmd}(k) = 0\,\text{deg}.\end{gathered} \tag{47}$$

At $t = 250$ sec, the cg is abruptly moved aft by 1.15 inch, and the mass and moments of inertia are abruptly decreased as in Example 3.

Figure 5 shows that, after the initial adaptation, the maximum command-following errors for airspeed, altitude, turn rate, and sideslip angle are 2.38 kt, 9.7 ft, 0.54 deg/sec, and 0.05 deg, respectively. Figure 5(f) shows that, at $t = 250$ sec, the elevator controller coefficients readapt due to the resulting change in dynamics, and the aircraft continues straight-line flight with constant airspeed and altitude. At $t = 350$ sec, the command-following errors for airspeed, altitude, turn rate, and sideslip angle are 0.14 kt, 1.21 ft, 0.02 deg/sec, and 0.0004 deg, respectively. Note that the requested actuator settings in all four channels become constant after 280 sec.

VI. Abrupt Changes in the Aerodynamic Coefficients

We now investigate a scenario where the lift and drag change abruptly during flight. To model the abrupt increase in drag and reduction in lift, we abruptly increase the aerodynamic force coefficient by 40% in the longitudinal-axis direction at 250 sec, and we abruptly decrease the aerodynamic force coefficient by 30% in the vertical-axis direction at 250 sec, respectively.

Example 5. Straight-line flight with constant airspeed and trapezoidal altitude commands. The incremental commands are given by

$$\begin{gathered}\delta h_{\rm cmd}(k) = \begin{cases} 0, & k < 1000, \\ \min\{200, 0.1(k-1000)\}\,\text{ft}, & k \geq 1000, \end{cases} \\ \delta V_{\rm AC,cmd}(k) = 0\,\text{kt},\ \delta\tau_{\rm cmd}(k) = 0\,\text{deg/sec},\ \delta\beta_{\rm cmd}(k) = 0\,\text{deg}.\end{gathered} \tag{48}$$

Note that the abrupt change in the aerodynamic coefficients at $t = 250$ sec occurs during the trapezoidal altitude command.

Figure 6 shows that, after the initial adaptation, the maximum command-following errors for airspeed, altitude, turn rate, and sideslip angle are 2.38 kt, 9.7 ft, 0.54 deg/sec, and 0.05 deg, respectively. Figure 6(f) shows that, at $t = 250$ sec, the elevator controller coefficients readapt due to the change in the aerodynamic coefficients, and the aircraft continues to follow the trapezoidal altitude command. At $t = 400$ sec, the command-following errors for airspeed, altitude, turn rate, and sideslip angle are 0.96 kt, 1.65 ft, 0.07 deg/sec, and 0.0008 deg, respectively.

Example 6. Straight-line flight with trapezoidal altitude command, followed by horizontal circular flight with trapezoidal turn-rate command and constant altitude command. The incremental commands are

given by

$$\delta h_{\rm cmd}(k) = \begin{cases} 0, & k < 1000, \\ \min\{100, 0.1(k-1000)\}\,\text{ft}, & k \geq 1000, \end{cases}$$
$$\delta\tau_{\rm cmd}(k) = \begin{cases} 0, & k < 3500, \\ \min\{5, 0.005(k-3500)\}\,\text{deg/sec}, & k \geq 3500, \end{cases} \tag{49}$$
$$\delta V_{\rm AC,cmd}(k) = 0\,\text{kt},\ \delta\beta_{\rm cmd}(k) = 0\,\text{deg},$$

where the trapezoidal altitude command starts at $t = 100$ sec, and the trapezoidal turn-rate command starts at $t = 350$ sec. Note that the abrupt change in the aerodynamic coefficients at $t = 250$ sec occurs before the trapezoidal turn-rate command.

Figure 7 shows that, after the initial adaptation, the maximum command-following errors for airspeed, altitude, turn rate, and sideslip angle are 2.19 kt, 11.14 ft, 2.4 deg/sec, and 0.12 deg, respectively. To compensate for the change in the aerodynamic coefficients, RCAC changes the throttle, elevator deflection, and aileron deflection from 22.8%, 2.69 deg, and 0.001 deg at $t = 250$ sec to 24.18%, 1.02 deg, and -0.003 deg at $t = 300$ sec, respectively. Figure 7(i) shows that, at $t = 350$ sec, the ailerons controller coefficients readapt to follow the trapezoidal turn-rate command. At $t = 500$ sec, the command-following errors for airspeed, altitude, turn rate, and sideslip angle are 1.86 kt, 2.55 ft, 0.0007 deg/sec, and 0.09 deg, respectively.

VII. Abrupt Control-Surface Deflection and Jam

Example 7. Horizontal circular flight with constant altitude and trapezoidal turn-rate commands. The incremental commands are given by

$$\delta\tau_{\rm cmd}(k) = \begin{cases} 0, & k < 2000, \\ \max\{-5, -0.005(k-2000)\}\,\text{deg/sec}, & k \geq 2000, \end{cases} \tag{50}$$
$$\delta V_{\rm AC,cmd}(k) = 0\,\text{kt},\ \delta h_{\rm cmd}(k) = 0\,\text{ft},\ \delta\beta_{\rm cmd}(k) = 0\,\text{deg},$$

where the trapezoidal turn-rate command starts at $t = 200$ sec. At $t = 100$ sec, the rudder angle abruptly changes by 2 deg and then jams. Note that the abrupt rudder-deflection occurs before the trapezoidal turn-rate command.

Figure 8 shows that, after the initial adaptation, the maximum command-following errors for airspeed, altitude, turn rate, and sideslip angle are 0.67 kt, 8.42 ft, 10.21 deg/sec, and 1.94 deg, respectively. Figure 8(i) shows that, at $t = 100$ sec, the ailerons controller coefficients readapt and the aircraft continues straight-line flight. To compensate for the abrupt change in rudder deflection, RCAC changes the throttle, elevator deflection, and aileron deflection from 22.86%, 2.7 deg, and 0.001 deg at $t = 100$ sec to 22.86%, 2.5 deg, and -1.93 deg at $t = 130$ sec, respectively. Figure 8(g) shows that, starting at $t = 200$ sec, RCAC is able to follow the turn-rate command with a jammed rudder. At $t = 350$ sec, the command-following errors for airspeed, altitude, turn rate, and sideslip angle are 0.56 kt, 1.29 ft, 0.18 deg/sec, and 1.38 deg, respectively.

Example 8. Horizontal circular flight with constant altitude and trapezoidal turn-rate commands. The incremental commands are given by

$$\delta\tau_{\rm cmd}(k) = \begin{cases} 0, & k < 1000, \\ \min\{5, 0.005(k-1000)\}\,\text{deg/sec}, & k \geq 1000, \end{cases} \tag{51}$$
$$\delta V_{\rm AC,cmd}(k) = 0\,\text{kt},\ \delta h_{\rm cmd}(k) = 0\,\text{ft},\ \delta\beta_{\rm cmd}(k) = 0\,\text{deg}.$$

where the trapezoidal turn-rate command starts at $t = 100$ sec. At $t = 250$ sec, the rudder angle abruptly changes by -2 deg and then jams. Note that the abrupt rudder deflection occurs during the horizontal circular flight.

Figure 9 shows that, after the initial adaptation, the maximum command-following errors for airspeed, altitude, turn rate, and sideslip angle are 1.67 kt, 10.61 ft, 10.03 deg/sec, and 2.23 deg, respectively. Figure 9(i) shows that, at $t = 250$ sec, the aileron controller coefficients readapt and the aircraft continues horizontal circular flight with constant altitude. To compensate for the abrupt change in rudder deflection, RCAC changes the throttle, elevator deflection, and aileron deflection from 23.47%, 2.19 deg, and -0.035 deg at $t = 250$ sec to 23.36%, 1.98 deg, and 1.95 deg at $t = 300$ sec, respectively. At $t = 350$ sec, the command-following errors for airspeed, altitude, turn rate, and sideslip angle are 0.51 kt, 1.05 ft, 0.21 deg/sec, and 1.44 deg, respectively.

VIII. Abrupt Thrust Failure

We now investigate a scenario involving an abrupt lost of thrust in one of the two engines. Under nominal conditions, RCAC uses equal thrust from both engines, that is, the requested actuator setting increments for the left and right engines are $\delta \boldsymbol{T}_{\rm req}$ and $\delta \boldsymbol{T}_{\rm req}$, respectively.

Example 9. Straight-line flight with constant altitude and trapezoidal airspeed commands. The incremental commands are given by

$$\delta V_{\rm AC,cmd}(k) = \begin{cases} 0, & k < 1000, \\ \max\{-10, -0.01(k-1000)\}\,\text{kt}, & k \geq 1000, \end{cases} \qquad (52)$$
$$\delta h_{\rm cmd}(k) = 0\,\text{ft},\ \delta\tau_{\rm cmd}(k) = 0\,\text{deg/sec},\ \delta\beta_{\rm cmd}(k) = 0\,\text{deg},$$

where the trapezoidal airspeed command starts at $t = 100$ sec. At $t = 250$ sec, the right engine fails, and thus $T_{\rm actual,right}$ is zero afterwards. Note that, after the right engine fails, there is an aileron compensation required to maintain zero turn-rate command, as well as, an additional thrust from the left engine to maintain the constant airspeed command.

Figure 10 shows that, after the initial adaptation, the maximum command-following errors for airspeed, altitude, turn rate, and sideslip angle are 10.86 kt, 3.82 ft, 3.3 deg/sec, and 1.7 deg, respectively. Figures 10(d),10(g),10(j),10(m) show that, at $t = 250$ sec, the throttle, elevator, ailerons, and rudder controller coefficients readapt and the aircraft continues straight-line flight with constant altitude. To compensate for the abrupt loss of the right-engine thrust, RCAC changes the left throttle, elevator deflection, aileron deflection, and rudder deflection from 19.93%, 1.92 deg, -0.002 deg, and 0.004 deg at $t = 250$ sec to 33.96%, 1.78 deg, 1.20 deg, and 0.59 deg at $t = 350$ sec, respectively. At $t = 450$ sec, the command-following errors for airspeed, altitude, turn rate, and sideslip angle are 0.11 kt, 0.89 ft, 0.14 deg/sec, and 0.58 deg, respectively.

IX. Conclusions

This paper extended the study in[1] by focusing on the application of retrospective cost adaptive control (RCAC) to aircraft faults that are abrupt, severe, unknown, and unforeseen. As in,[1] the present study is based on the fully nonlinear GTM model with extremely limited nominal modeling information. Nine scenarios were considered, including 1) abrupt changes in the aircraft mass properties; 2) abrupt changes in the aerodynamic coefficients; 3) abrupt control-surface deflection and jam; and 4) abrupt thrust failure. Since RCAC is a direct adaptive control technique, no attempt is made to explicitly learn and model the unknown fault. In order to reflect the assumption that the abrupt faults are unknown and unforeseen, the same tuning parameters were used for all applications of RCAC. In all cases, RCAC was able to re-adapt the controller coefficients in order to overcome the effect of the abrupt fault.

Acknowledgments

This research was supported in part by the Office of Naval Research under grant N00014-14-1-0596.

References

[1]A. Ansari and D. S. Bernstein. Retrospective Cost Adaptive Control of the Generic Transport Model Under Uncertainty and Failure. *Journal of Aerospace Information Systems*, 14(3):123–174, 2017.

[2]J. H. Blakelock. *Automatic Control of Aircraft and Missiles*. John Wiley & Sons, 1991.

[3]R. C. Nelson. *Flight Stability and Automatic Control*. WCB/McGraw Hill, 1998.

[4]D. T. McRuer, D. Graham, and I. Ashkenas. *Aircraft Dynamics and Automatic Control*. Princeton University Press, 2014.

[5]B. L. Stevens, F. L. Lewis, and E. N. Johnson. *Aircraft Control and Simulation: Dynamics, Controls Design, and Autonomous Systems*. John Wiley & Sons, 2015.

[6]A. Tewari. *Advanced Control of Aircraft, Spacecraft and Rockets*. John Wiley & Sons, 2011.

[7]R. J. Adams, J. M. Buffington, A. G. Sparks, and S. S. Banda. *Robust Multivariable Flight Control*. Springer, 2012.

[8]E. Lavretsky and K. Wise. *Robust and Adaptive Control: With Aerospace Applications*. Springer, 2012.

[9]N. Nguyen, K. Krishnakumar, J. Kaneshige, and P. Nespeca. Dynamics and Adaptive Control for Stability Recovery of Damaged Asymmetric Aircraft. In *Proc. AIAA Guid. Nav. Cont. Conf.*, pages 21–24, Keystone, CO, 2006. AIAA-2006-6049.

[10]N. T. Nguyen, K. S. Krishnakumar, J. T. Kaneshige, and P. P. Nespeca. Flight Dynamics and Hybrid Adaptive Control of Damaged Aircraft. *AIAA J. Guid. Contr. Dyn.*, 31:751–764, 2008.

[11]Y. Liu, G. Tao, and S. M. Joshi. Modeling and Model Reference Adaptive Control of Aircraft with Asymmetric Damage. *AIAA J. Guid. Contr. Dyn.*, 33:1500–1517, 2010.

[12]V. Stepanyan, K. Krishnakumar, and N. Nguyen. Adaptive Control of a Transport Aircraft Using Differential Thrust. *NASA Ames Research Center, Moffett Field, CA. NASA Publication*, 2009.

[13]Z. T. Dydek, A. M. Annaswamy, and E. Lavretsky. Adaptive Control and the NASA X-15-3 Flight Revisited. *IEEE Control Systems*, 30(3):32–48, 2010.

[14]N. Hovakimyan, C. Cao, E. Kharisov, E. Xargay, and I. M. Gregory. L1 Adaptive Control for Safety-Critical Systems. *IEEE Control Systems*, 31(5):54–104, 2011.

[15]Y. Rahman, A. Xie, and D. S. Bernstein. Retrospective Cost Adaptive Control: Pole Placement, Frequency Response, and Connections with LQG Control. *IEEE Contr. Sys. Mag.*, 37:28–69, October 2017.

[16]R. Venugopal and D. S. Bernstein. Adaptive Disturbance Rejection Using ARMARKOV System Representations. *IEEE Trans. Contr. Sys. Tech.*, 8:257–269, 2000.

[17]M. A. Santillo and D. S. Bernstein. Adaptive Control Based on Retrospective Cost Optimization. *AIAA J. Guid. Contr. Dyn.*, 33:289–304, 2010.

[18]J. B. Hoagg and D. S. Bernstein. Retrospective Cost Model Reference Adaptive Control for Nonminimum-Phase Systems. *J. Guid. Contr. Dyn.*, 35:1767–1786, 2012.

[19]S. Dai, Z. Ren, and D. S. Bernstein. Adaptive Control of Nonminimum-Phase Systems Using Shifted Laurent Series. *Int. J. Contr.*, 90:409–422, 2017.

[20]A. Ansari and D. S. Bernstein. Adaptive Control of an Aircraft with Uncertain Nonminimum-Phase Dynamics. In *Proc. Amer. Contr. Conf.*, pages 844–849, Chicago, IL, 2015.

[21]T. Jordan, W. Langford, C. Belcastro, J. Foster, G. Shah, G. Howland, and R. Kidd. Development of a Dynamically Scaled Generic Transport Model Testbed for Flight Research Experiments. *AUVSI Unmanned Unlimited, Arlington, VA*, 2004.

[22]R. M. Bailey, R. W. Hostetler, K. N. Barnes, C. Belcastro, and C. Belcastro. Experimental Validation: Subscale Aircraft Ground Facilities and Integrated Test Capability. In *Proc. AIAA Guid. Nav. Cont. Conf.*, page 110, San Francisco, CA, 2005. AIAA-2005-6433.

[23]T. L. Jordan and R. M. Bailey. NASA Langleys AirSTAR Testbed: A Subscale Flight Test Capability for Flight Dynamics and Control System Experiments. In *Proc. AIAA Guid. Nav. Cont. Conf.*, pages 18–21, Honolulu, HI, 2008. AIAA-2008-6660.

[24]K. Cunningham, D. E. Cox, D. G. Murri, and S. E. Riddick. A Piloted Evaluation of Damage Accommodating Flight Control Using a Remotely Piloted Vehicle. In *Proc. AIAA Guid. Nav. Cont. Conf.*, Portland, OR, 2011. AIAA-2011-6451.

[25]M. J. Yu, Y. Rahman, E. M. Atkins, I. Kolmanovsky, and D. S. Bernstein. Minimal Modeling Adaptive Control of the NASA Generic Transport Model with Unknown Control-Surface Faults. In *Proc. AIAA Guid. Nav. Contr. Conf.*, Boston, MA, 2013. AIAA-2013-4693.

[26]F. Sobolic and D. S. Bernstein. Aerodynamic-Free Adaptive Control of the NASA Generic Transport Model. In *Proc. AIAA Guid. Nav. Contr. Conf.*, Boston, MA, 2013. AIAA-2013-4999.

[27]A. Ansari, A. Prach, and D. S. Bernstein. Adaptive Trim and Trajectory Following for a Tilt-Rotor Tricopter. In *American Control Conference (ACC), 2017*, pages 1109–1114. IEEE, 2017.

[28]A. Ansari, M. J. Yu, and D. S. Bernstein. Exploration and Mapping of an Unknown Flight Envelope. In *Proc. Dyn. Sys. Contr. Conf.*, pages 523–528, Los Angeles, CA, 2014.

[29]D. Cox. GTM DesignSim: The Generic Transport Model. `https://github.com/nasa/GTM_DesignSim`, 2008.

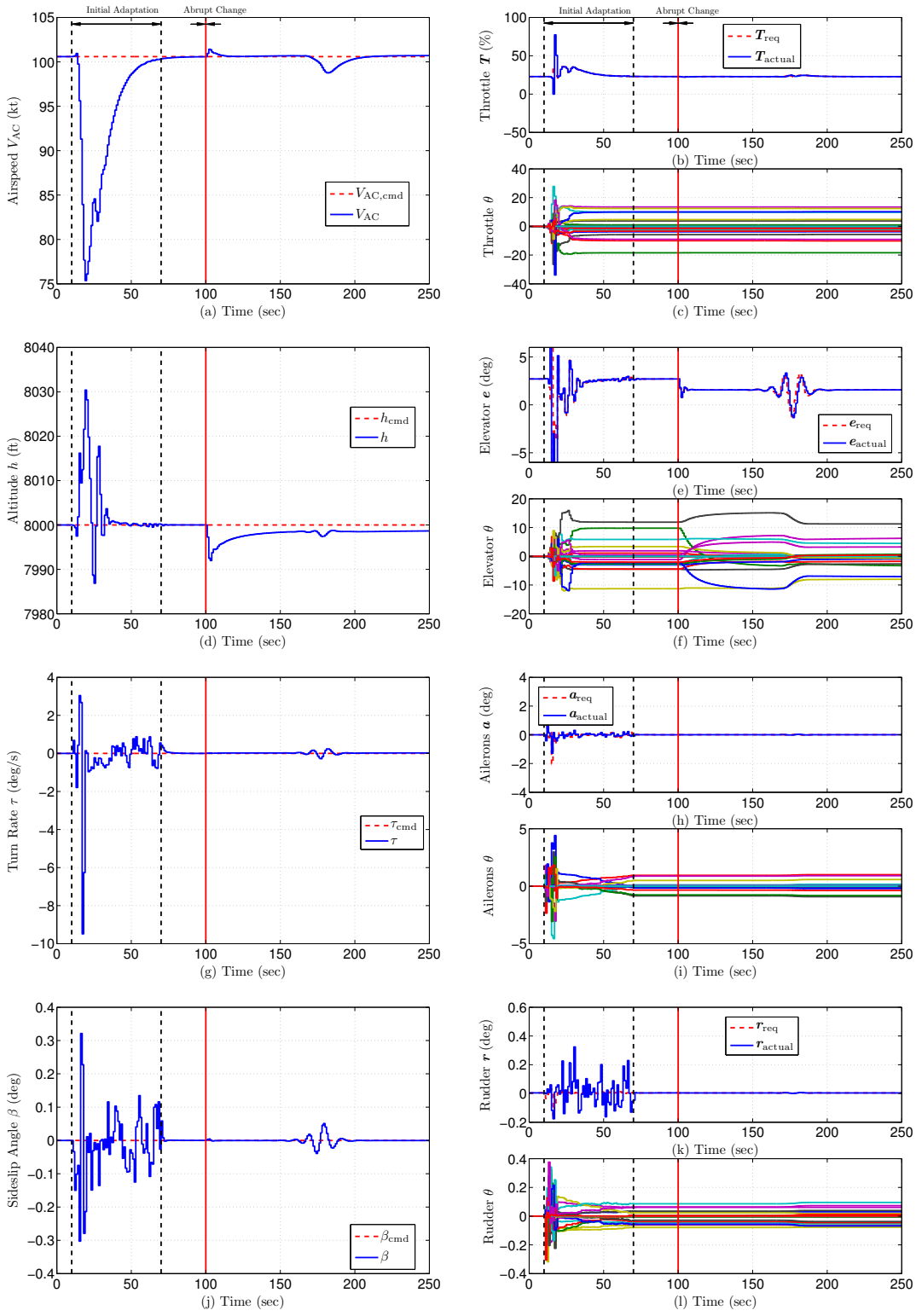

Figure 2. Straight-line flight with constant altitude and airspeed commands. Note that, from $t = 10$ to 70 sec, the transients are due to the initial adaptation. At $t = 100$ sec, the cg abruptly moves forward by 1.14 inch. Due to the resulting change in dynamics, the elevator controller coefficients readapt after $t = 100$ sec, and the aircraft continues straight-line flight with constant airspeed and altitude. At $t = 250$ sec, the command-following errors for airspeed, altitude, turn rate, and sideslip angle are 0.1 kt, 1.37 ft, 0.02 deg/sec, and 0.0003 deg, respectively.

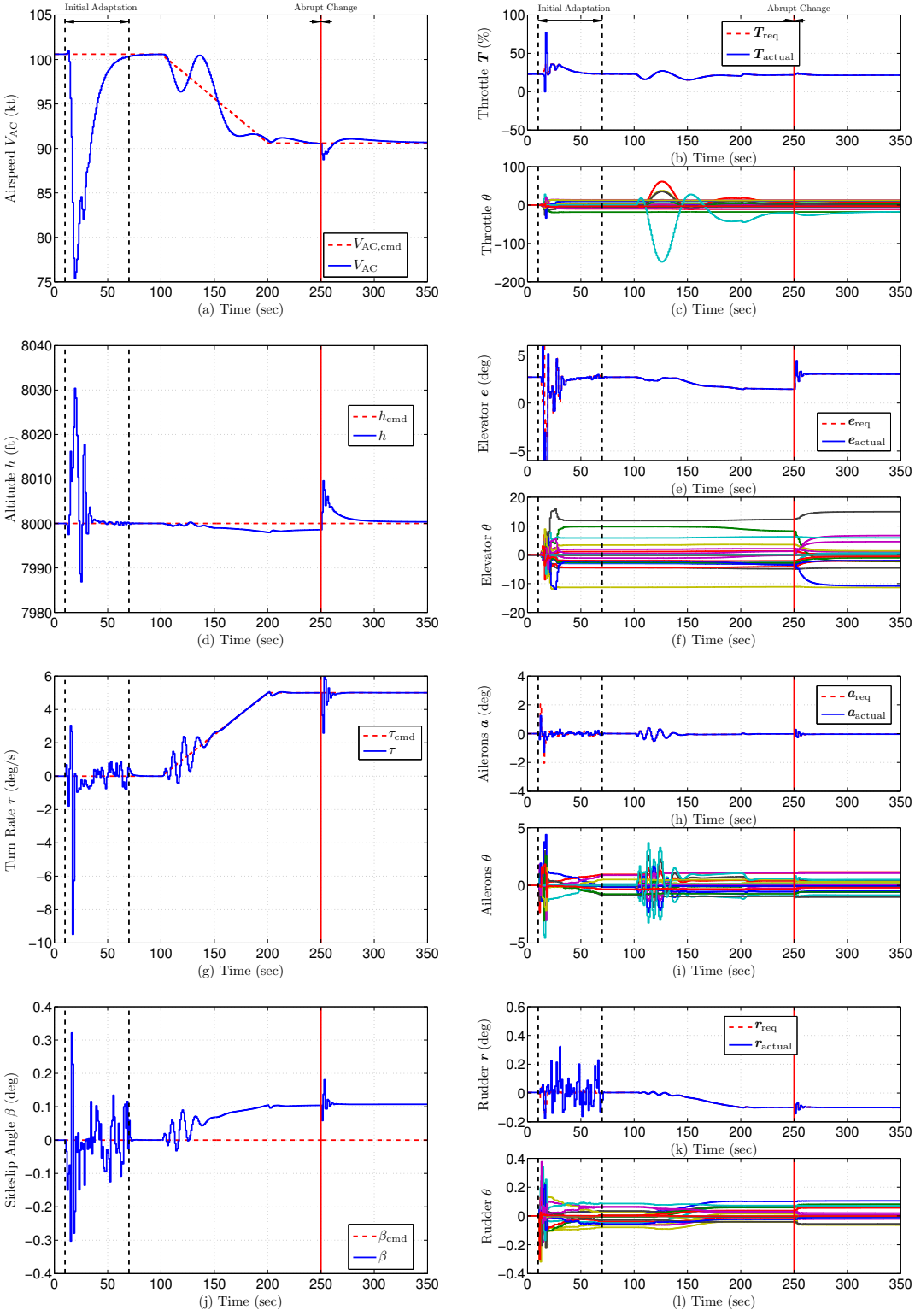

Figure 3. Horizontal circular flight with trapezoidal airspeed and turn-rate commands. After the initial adaptation, the maximum command-following errors for airspeed, altitude, turn rate, and sideslip angle are 3.54 kt, 9.56 ft, 2.41 deg/sec, and 0.18 deg, respectively. At $t = 250$ sec, the cg abruptly moves aft by 1.15 inch. Due to the resulting change in dynamics, the elevator controller coefficients readapt after $t = 250$ sec, and the aircraft continues horizontal circular flight with constant airspeed and altitude. Note that the requested actuator settings in all four channels become constant after 280 sec. At $t = 350$ sec, the command-following errors for airspeed, altitude, turn rate, and sideslip angle are 0.1 kt, 0.35 ft, 0.002 deg/sec, and 0.10 deg, respectively.

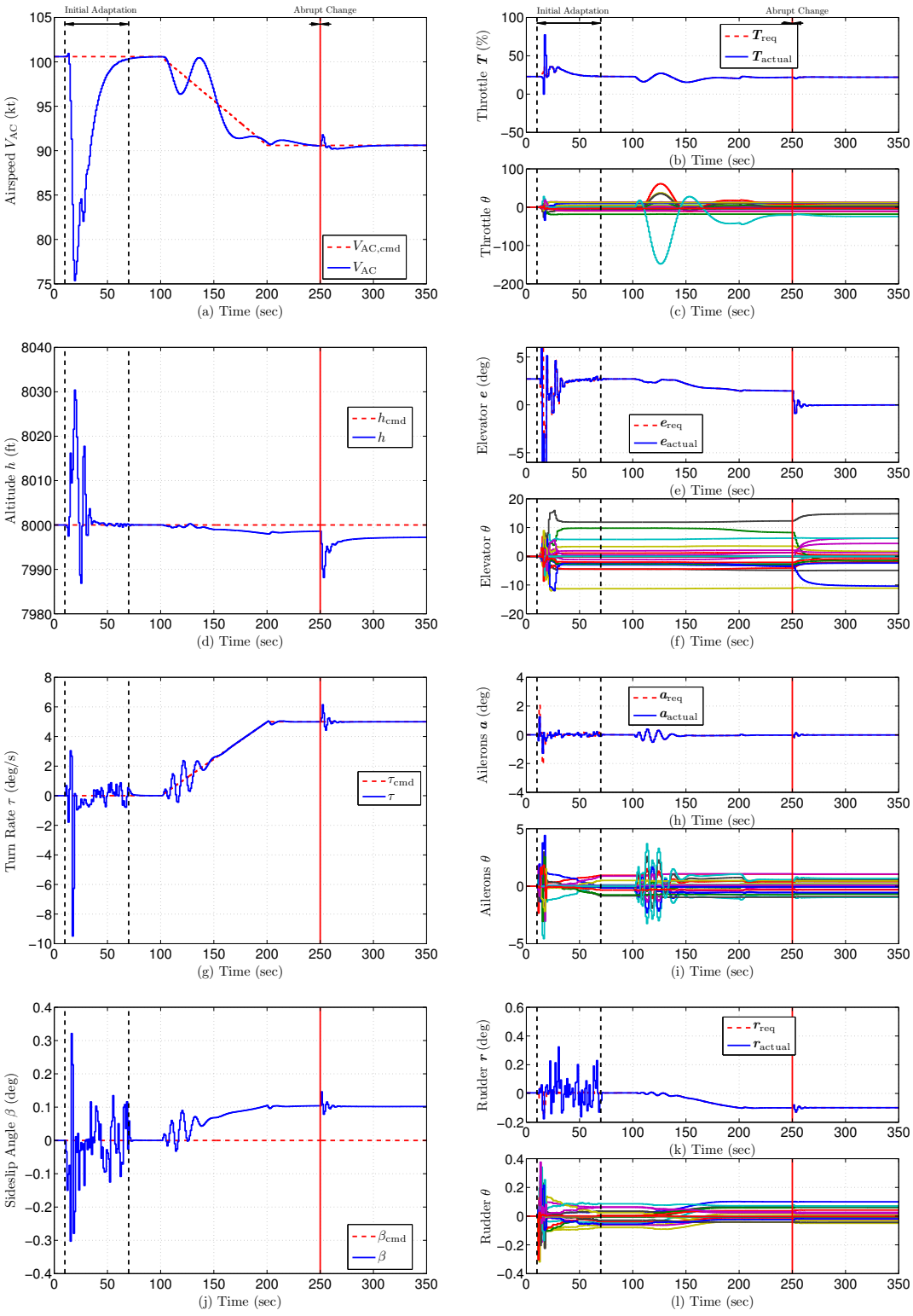

Figure 4. Horizontal circular flight with trapezoidal airspeed and turn-rate commands. After the initial adaptation, the maximum command-following errors for airspeed, altitude, turn rate, and sideslip angle are 3.55 kt, 11.84 ft, 1.32 deg/sec, and 0.14 deg, respectively. At $t = 250$ sec, the cg abruptly moves forward, and the mass and moment of inertial abruptly decreases. Due to the resulting change in dynamics, the elevator controller coefficients readapt after $t = 250$ sec, and the aircraft continues horizontal circular flight with constant airspeed and altitude. Note that the requested actuator settings in all four channels become constant after 280 sec. At $t = 300$ sec, the command-following errors for airspeed, altitude, turn rate, and sideslip angle are 0.01 kt, 2.8 ft, 0.002 deg/sec, and 0.10 deg, respectively.

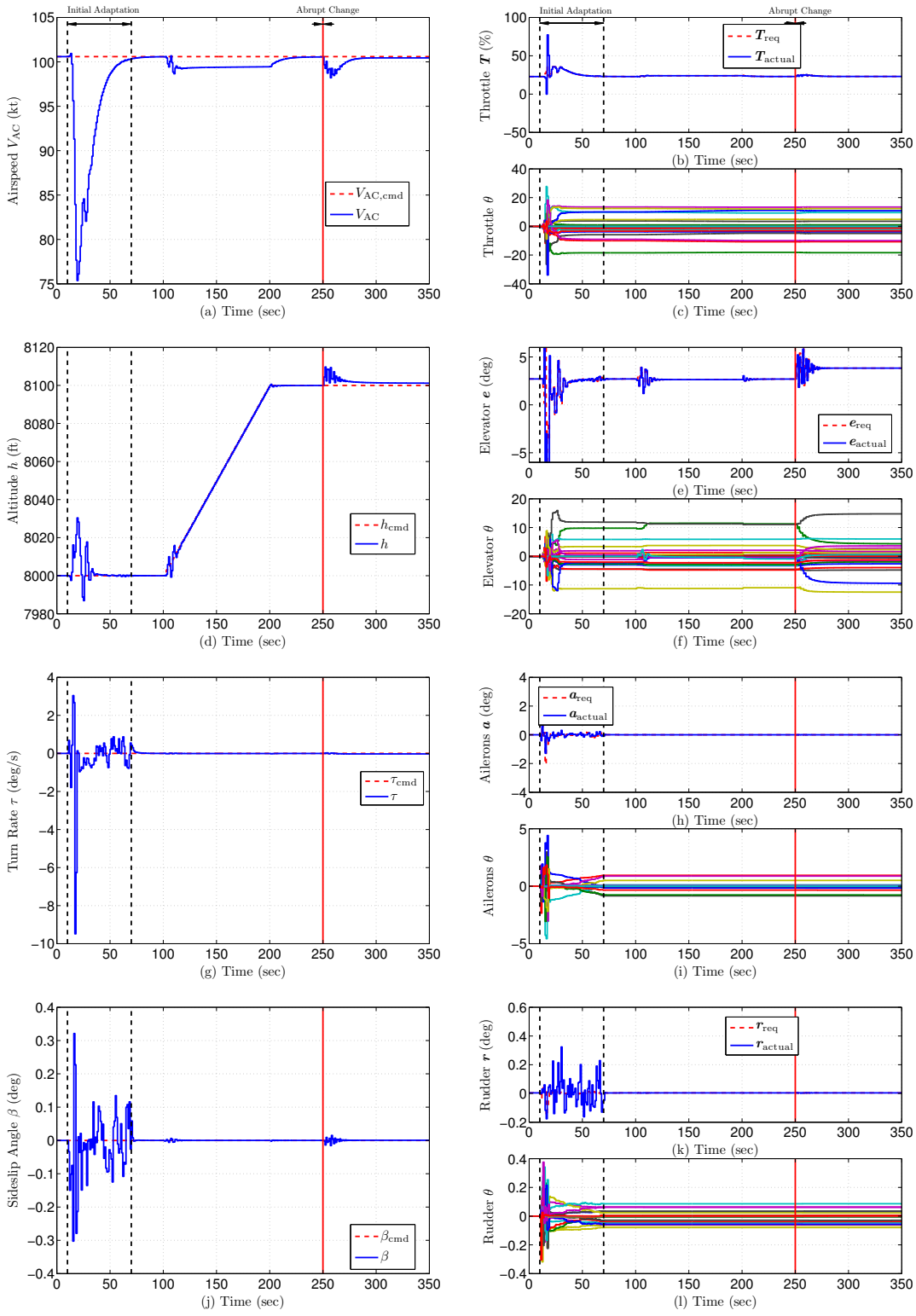

Figure 5. Straight-line flight with constant airspeed and trapezoidal altitude commands. After the initial adaptation, the maximum command-following errors for airspeed, altitude, turn rate, and sideslip angle are 2.38 kt, 9.7 ft, 0.54 deg/sec, and 0.05 deg, respectively. At $t = 250$ sec, the cg abruptly moves aft, and the mass and moment of inertial abruptly decreases. Due to the resulting change in dynamics, the elevator controller coefficients readapt after $t = 250$ sec, and the aircraft continues straight-line flight with constant airspeed and altitude. Note that the requested actuator settings in all four channels become constant after 280 sec. At $t = 300$ sec, the command-following errors for airspeed, altitude, turn rate, and sideslip angle are 0.14 kt, 1.21 ft, 0.02 deg/sec, and 0.0004 deg, respectively.

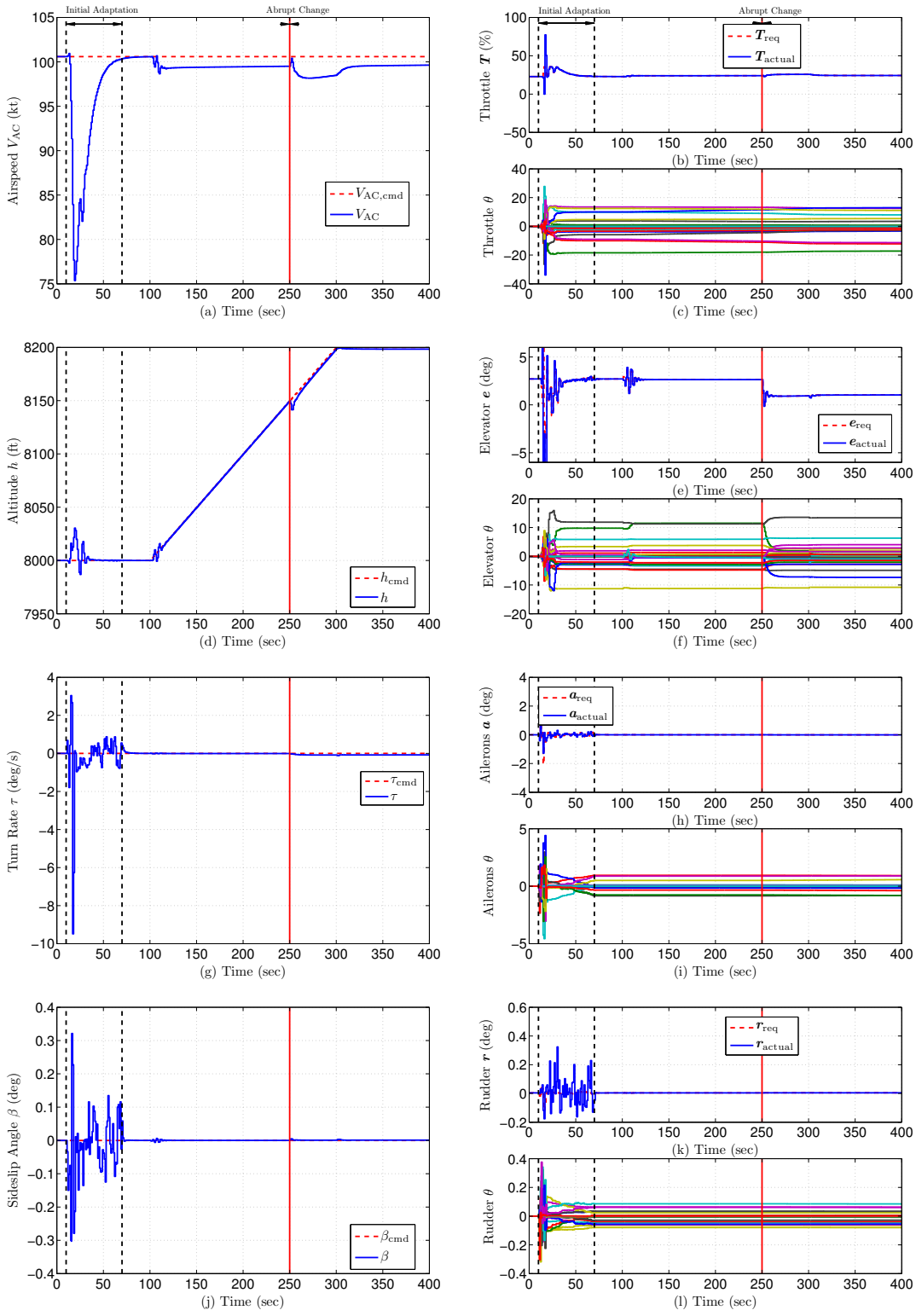

Figure 6. Straight-line flight with constant airspeed and trapezoidal altitude commands. After the initial adaptation, the maximum command-following errors for airspeed, altitude, turn rate, and sideslip angle are 2.38 kt, 9.7 ft, 0.54 deg/sec, and 0.05 deg, respectively. Note that the abrupt change in the aerodynamic coefficients at $t = 250$ sec occurs during the trapezoidal altitude command. Due to the resulting change in dynamics, the elevator controller coefficients readapt after $t = 250$ sec, and the aircraft continues to follow the trapezoidal altitude command. At $t = 300$ sec, the command-following errors for airspeed, altitude, turn rate, and sideslip angle are 0.96 kt, 1.65 ft, 0.07 deg/sec, and 0.0008 deg, respectively.

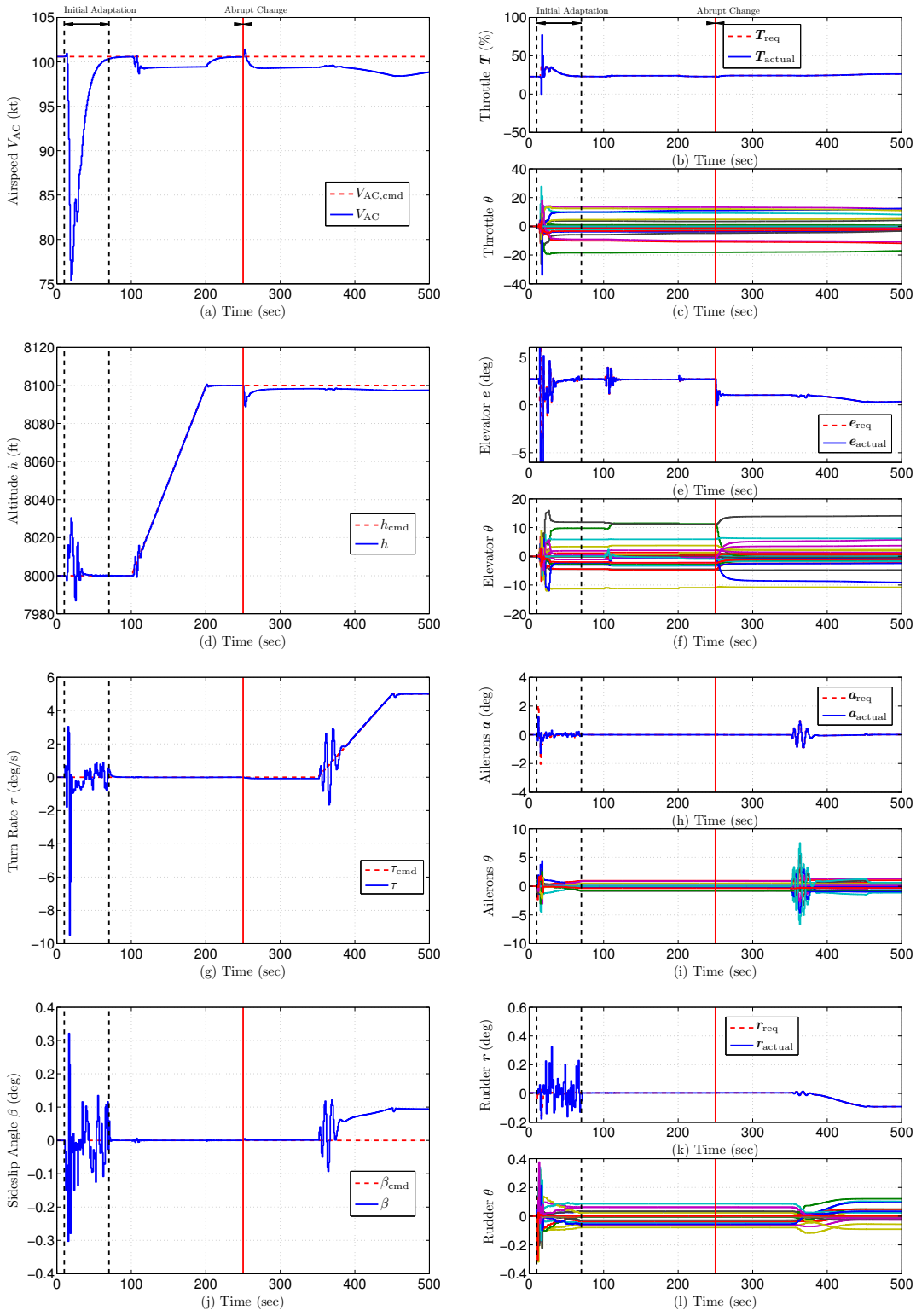

Figure 7. Straight-line flight with trapezoidal altitude command, followed by horizontal circular flight with trapezoidal turn-rate command and constant altitude command. Note that the abrupt change in the aerodynamic coefficients at $t = 250$ sec occurs before the trapezoidal turn-rate command. To compensate for the change in the aerodynamic coefficients, RCAC changes the throttle, elevator deflection, and aileron deflection from 22.8%, 2.69 deg, and 0.001 deg at $t = 250$ sec to 24.18%, 1.02 deg, and -0.003 deg at $t = 300$ sec, respectively. At $t = 350$ sec, the ailerons controller coefficients readapt to follow the trapezoidal turn-rate command. At $t = 500$ sec, the command-following errors for airspeed, altitude, turn rate, and sideslip angle are 1.86 kt, 2.55 ft, 0.0007 deg/sec, and 0.09 deg, respectively.

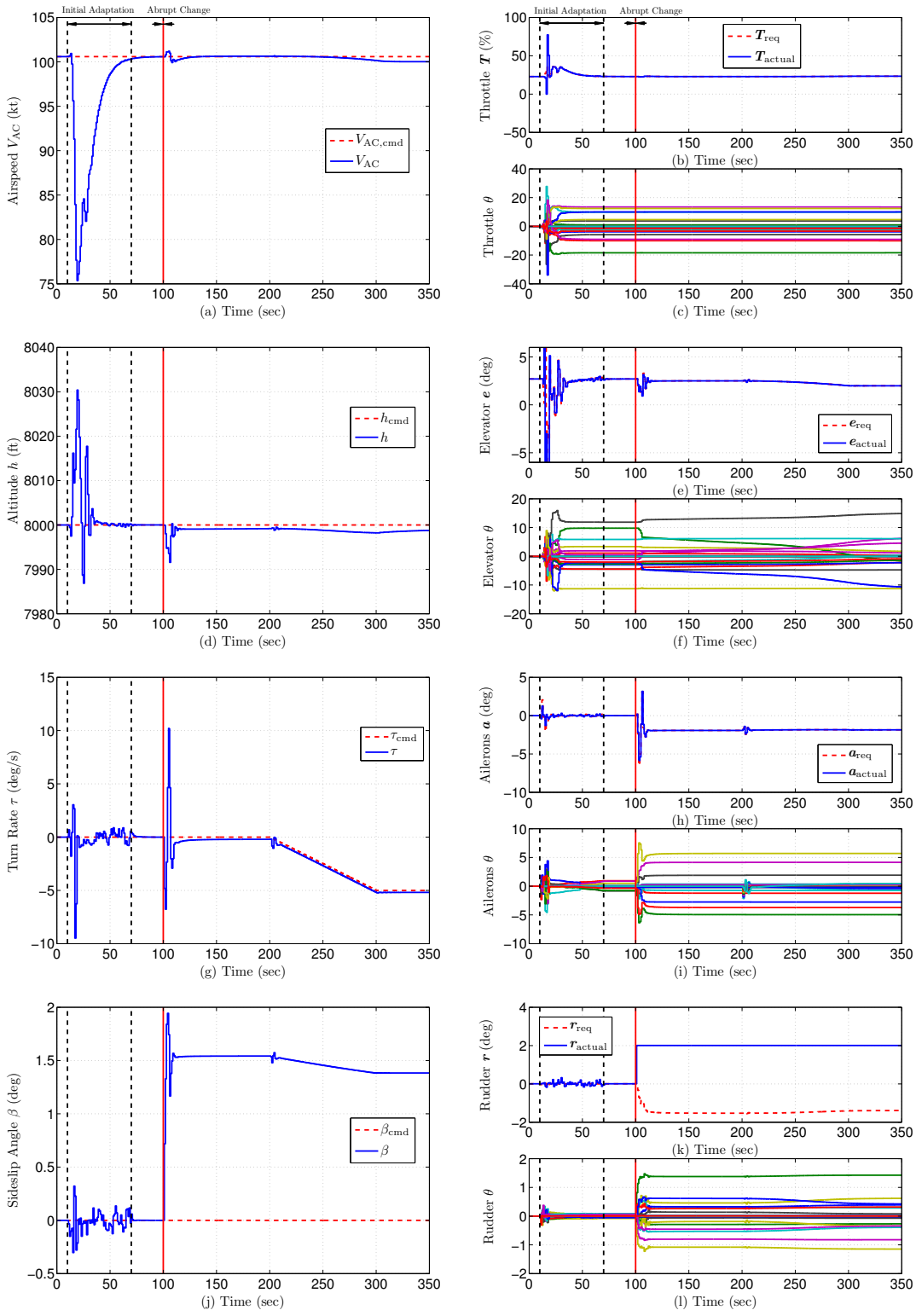

Figure 8. Horizontal circular flight with constant altitude and trapezoidal turn-rate commands. At $t = 100$ sec, the rudder abruptly moves by 2 deg and then jams. To compensate for the abrupt change in rudder deflection, RCAC changes the throttle, elevator deflection, and aileron deflection from 22.86%, 2.7 deg, and 0.001 deg at $t = 100$ sec to 22.86%, 2.5 deg, and -1.93 deg at $t = 130$ sec, respectively. Note that, starting at $t = 200$ sec, RCAC is able to follow the turn-rate command with a jammed rudder. At $t = 350$ sec, the command-following errors for airspeed, altitude, turn rate, and sideslip angle are 0.56 kt, 1.29 ft, 0.18 deg/sec, and 1.38 deg, respectively.

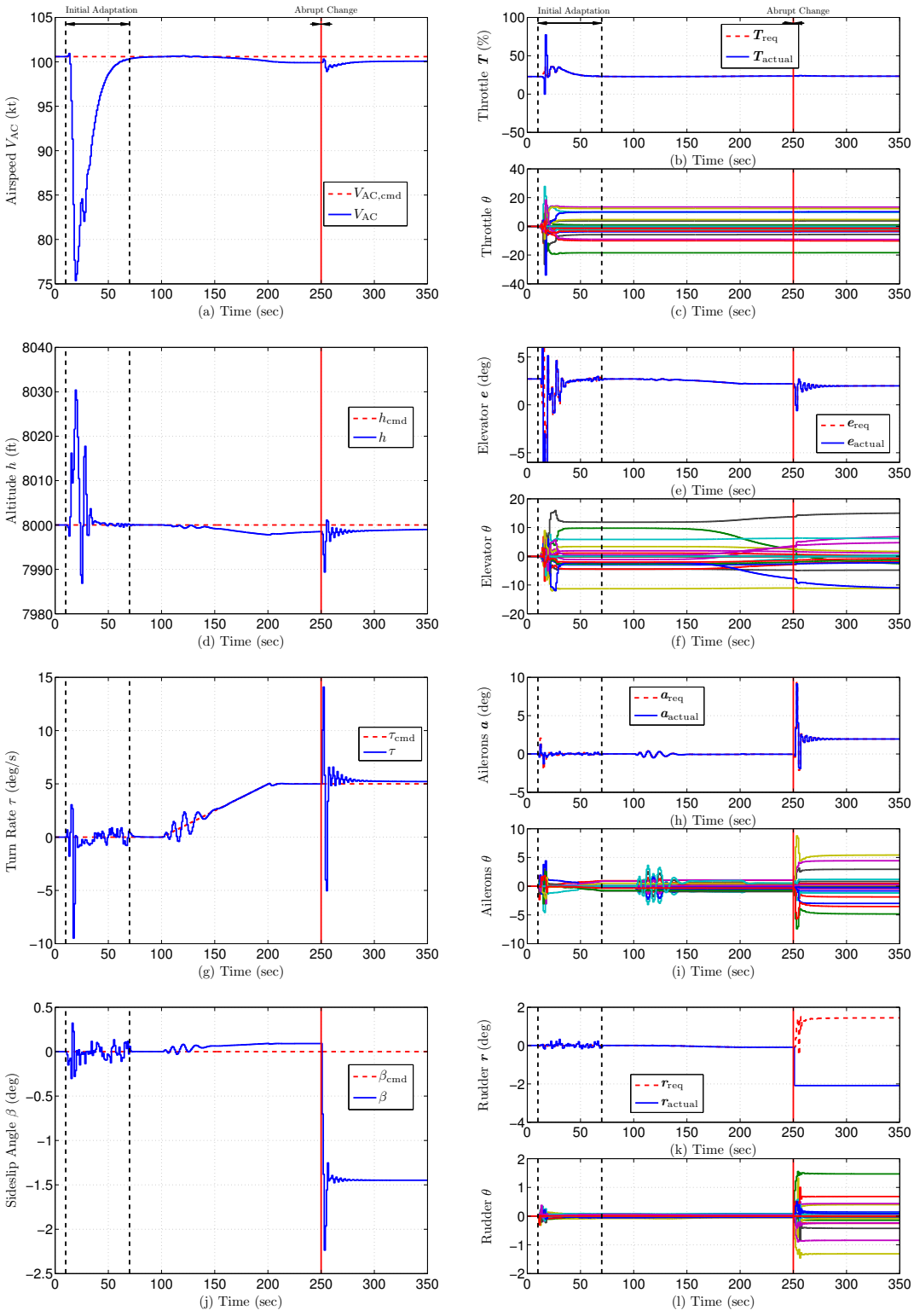

Figure 9. Horizontal circular flight with constant altitude and trapezoidal turn-rate commands. At $t = 100$ sec, the rudder abruptly moves by -2 deg and then jams. At $t = 250$ sec, the ailerons controller coefficients readapt and the aircraft continues horizontal circular flight with constant altitude. To compensate for the abrupt change in rudder deflection, RCAC changes the throttle, elevator deflection, and aileron deflection from 23.47%, 2.19 deg, and -0.035 deg at $t = 250$ sec to 23.36%, 1.98 deg, and 1.95 deg at $t = 300$ sec, respectively. At $t = 350$ sec, the command-following errors for airspeed, altitude, turn rate, and sideslip angle are 0.51 kt, 1.05 ft, 0.21 deg/sec, and 1.44 deg, respectively.

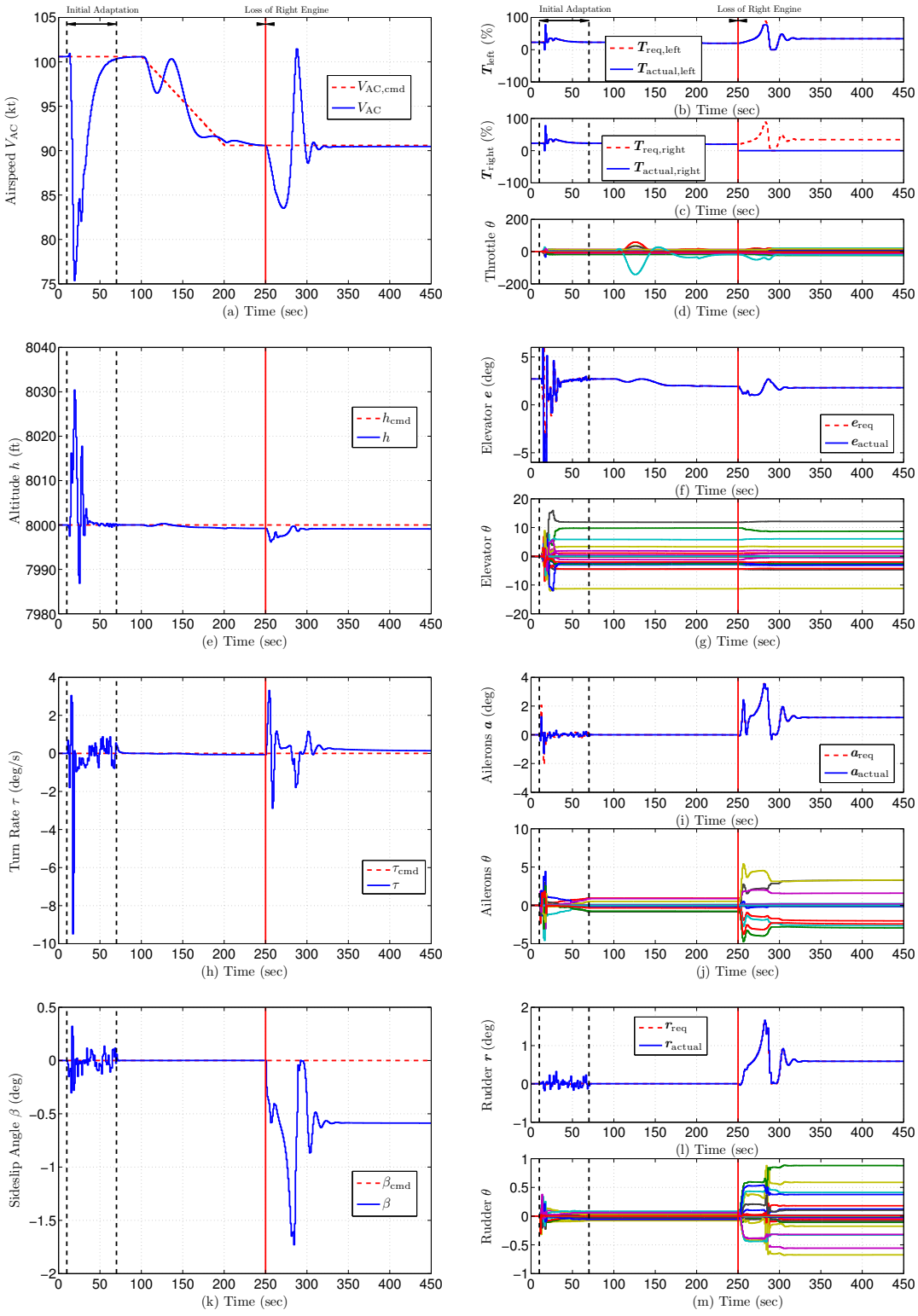

Figure 10. Straight-line flight with constant altitude and trapezoidal airspeed commands. At $t = 250$ sec, the right engine fails, and thus $T_{\text{actual,right}}$ is zero afterwards. To compensate for the abrupt loss of right engine's thrust, RCAC changes the left throttle, elevator deflection, aileron deflection, and rudder deflection from 19.93%, 1.92 deg, -0.002 deg, and 0.004 deg at $t = 250$ sec to 33.96%, 1.78 deg, 1.20 deg, and 0.59 deg at $t = 350$ sec, respectively. At $t = 450$ sec, the command-following errors for airspeed, altitude, turn rate, and sideslip angle are 0.11 kt, 0.89 ft, 0.14 deg/sec, and 0.58 deg, respectively.